ORIGINAL ARTICLE

Cisplatin cycles treatment sustains cardiovascular and renal damage involving TLR4 and NLRP3 pathways

Antonio González[1,2,3] | Soledad García-Gómez-Heras[1,3] | Raquel Franco-Rodríguez[1] | Visitación López-Miranda[1,2,3] | Esperanza Herradón[1,2,3]

[1]Departamento de Ciencias Básicas de la Salud, Facultad de Ciencias de la Salud, Universidad Rey Juan Carlos, Alcorcón, Spain

[2]Unidad Asociada al Instituto de Química Medica (IQM) del Consejo Superior de Investigaciones Científicas (CSIC), Universidad Rey Juan Carlos, Alcorcón, Spain

[3]High Performance Research Group in Experimental Pharmacology (Pharmakom-URJC), URJC, Alcorcón, Spain

Correspondence
Visitación López-Miranda, Departamento de Ciencias Básicas de la Salud, Facultad de Ciencias de la Salud, Universidad Rey Juan Carlos, Alcorcón, Madrid, Spain.
Email: visitacion.lopezmiranda@urjc.es

Abstract

Cisplatin is clinically proven to combat different cancers, including sarcomas, soft tissue cancers, bones, muscles, and blood. However, renal and cardiovascular toxicities are important limitations in cisplatin therapeutical use. Immunoinflammation could be key factor in cisplatin-induced toxicity. The aim of the present study was to evaluate the activation of the inflammatory TLR4/NLRP3 pathway as a common mechanism for cardiovascular and renal cisplatin's cycles treatment toxicity. Adult male Wistar rats were treated with saline, cisplatin 2 mg/kg or cisplatin 3 mg/kg (intraperitoneally once a week, for five experimental weeks). After treatments, plasma, cardiac, vascular, and renal tissues were collected. Plasma malondialdehyde (MDA) and inflammatory cytokines were determined. TLR4, MyD88, NF-κβ p65, NLRP3, and procaspase-1 tissue expressions were also analyzed. Cisplatin treatment induced a dose-dependent increase in plasma MDA and IL-18. In cardiovascular system, an increase in NLRP3 and in cleaved caspase-1 were observed in cardiac tissue and a moderate increase in TLR4, MyD88 appeared in mesenteric artery. In kidney, a significant dose-dependent increase in TLR4, MyD88 and NLRP3 and cleaved caspase 1 expressions were observed after cisplatin treatments. In conclusion, cisplatin cycles provoke a low grade pro-inflammatory systemic state. Kidney was more sensitive than cardiovascular tissues to this pro-inflammatory state. TLR4 and NLRP3 are key pathways involved in renal tissue damage, NLRP3 is the main pathway involved in cardiac toxicity and TLR4 pathway in resistance vessel toxicity.

KEYWORDS
cardiovascular toxicity, cisplatin cycles, NLRP3, renal damage, TLR4

1 | INTRODUCTION AND BACKGROUND

Cisplatin is one of the most effective anticancer drugs widely used in the treatment of solid tumors. It has been extensively used for the cure of different types of neoplasms including head and neck, lung, ovarian, leukemia, breast, brain, kidney, and testicular cancers. Cisplatin is considered as a cytotoxic drug in cancer cells which provokes damage in DNA, inhibiting DNA synthesis and mitosis, and inducing apoptotic cell death.[1]

However, toxic side effects of cisplatin are the main limitations of their use for the treatment of malignancy tumors and include nephrotoxicity, cardiotoxicity, myelotoxicity, ototoxicity, hepatotoxicity, and gastrointestinal toxicity.[2,3]

Cisplatin-related nephrotoxicity is a major limiting factor in its therapy since about 20% of the patients that receive cisplatin develop renal damage. Nephrotoxicity is due to the absorption by proximal tubular cells, and that leads to renal pathophysiological disorders.[3,4] On the other hand, it is suggested that cisplatin produces injury mainly in myocardial cells and vascular endothelium and eventually leads to myocardial cell systolic dysfunction associated with mitochondrial damage and vascular endothelial injury.[2,5]

The main known mechanism for cisplatin-induced cardiac and renal toxicities is its ability to shift the redox balance in cells by conjugation, and thereby depletion of the antioxidant glutathione and impairment of mitochondrial respiration, leading to excessive reactive oxygen species (ROS) formation. This induces a cascade of events leading to activation of different inflammatory pathways, and ultimately cell death.[6,7] In different cisplatin rodent models of cardiac and renal toxicity, inflammation plays a decisive role in the progression of cisplatin-induced toxicity.[3,7–11] However, the exact mediators and mechanisms involved in this inflammatory damage remain elusive.

Recently, it is being pointed out that cisplatin-induced cellular damage and necrosis leads to the release of damage-associated molecular patterns which activate pattern recognition receptors from the innate immune system. It has been also described that chronic inflammation mediated by these receptors plays a role in the development of cardiovascular diseases, being inflammatory responses one of the factors that could aggravate structural and/or pathological changes.[12–15] Among the possible targets involved in this immunoinflammatory damage, the toll-like receptor 4 (TLR4) and the nucleotide oligomerization domain-like receptor protein 3 (NLRP3) inflammasome stand out.

Previous studies of our group have shown that chronic cisplatin treatment, in cycles, provokes cardiac and vascular toxicity in a dose-dependent manner. Moreover, vascular endothelial dysfunction occurs at lower doses than cardiac and systemic cardiovascular toxicity. Besides, some structural changes in cardiac and vascular tissues are also patent even before any systemic cardiovascular alterations.[16] The aim of the present study was to evaluate if the activation of the inflammatory TLR4/MyD88/NLRP3 pathway and the production of proinflammatory cytokines are related with the cardiac, vascular, and renal toxicity caused by chronic cisplatin administration. The identification of these common targets as possible culprits would allow the design of treatment strategies aimed at avoiding them simultaneously.

2 | MATERIALS AND METHODS

The study was conducted in accordance with the Guide for the Care and Use of Laboratory Animals as adopted and promulgated by the U.S. National Institutes of Health.[17]

2.1 | Ethics statement

Experimental procedures were carried out in accordance with the recommendations of the Ethical Committee of the Universidad Rey Juan Carlos as well as with the EU directive for the protection of animals used for scientific purpose (2010/63/UE) and Spanish regulations (RD 109 53/2013).

2.2 | Animals

Male Wistar rats [240–300 g, Harlan-Iberica (Barcelona, Spain)] were placed in cages (4–6 animals) and maintained in environmentally controlled conditions (temperature of 20°C; humidity of 60%) with a 12 h light/12 h dark cycle. Animals had free access to standard laboratory rat chow (Harlan-Iberica, Barcelona) and tap water, which was refreshed every day.

2.3 | Treatments

After an adaptation period, the animals were divided into three treatment groups (10–15 animals per group): saline (0.9% NaCl) and cisplatin (2 and 3 mg/kg, cumulative dose of 10 and 15 mg/kg respectively). Saline or cisplatin was administered intraperitoneally once a week for five experimental weeks following experimental procedure described by Authier.[18] This administration schedule mimics cycle therapy in humans.

Cisplatin doses were chosen based on the commonly used in experimental protocols in rats to induce a wide range of toxic effects caused by this anticancer agent that also are observed in humans.[18,19]

At the end of the study, the rats were anesthetized (50 mg/kg i.p. sodium pentobarbital) and blood was collected into tubes containing lithium heparin as an anticoagulant. These samples were centrifuged to obtain plasma, which was divided into aliquots and kept frozen at −80°C until analysis. Hearts were excised, and left ventricles were isolated, followed by aorta and mesenteric bed excision. Left kidney were excised, and the coronal section of the whole kidney were separated into two sections. A small part of all tissues was preserved in 10% neutral buffered-fomalin for immunohistochemistry.

2.4 | Measurement of malondialdehyde (MDA) production

To evaluate oxidative stress, plasma MDA levels were measured by a modified thiobarbituric acid assay described by Alvarez et al.[20]

2.5 | Plasma inflammatory marker multiplex analysis

Systemic protein levels of cytokines/chemokines and grow factors in the plasma were assessed using the Bio-Plex MAGPIX, based on the Luminex assay. The levels of cytokines were detected in the present study by using a Bio-Plex Pro™ Rat Cytokine Group I 23-plex kit (BioRad, Cat#12005641) which included 23 cytokines (granulocyte colony-stimulating factor (G-CSF), granulocyte-macrophage (GM)-CSF, chemokine (C-X-C motif) ligand 1 (GRO/KC), interferon (IFN)-γ, IL-1α, IL-1β, IL-2, IL-5, IL-6, IL-4, IL-7, IL-10, IL-12p70, IL-13, IL-17A, IL18, macrophage colony-stimulating factor (M-CSF), monocyte chemoattractant protein-1 (MCP-1), macrophage colony-stimulating factor (M-CSF), macrophage inflammatory protein (MIP) MIP-1α, MIP-3α, C-C motif chemokine ligand 5 (RANTES), tumor necrosis factor-α (TNF-α), and vascular endothelial grow factor (VEGF)). Each experiment was performed in duplicate. The levels of these cytokines were calculated via Bio-Plex Pro™ software (Bio-Rad Laboratories, Inc.). Standard curves for each cytokine were generated using a kit-supplied reference cytokine sample.[21]

After the determination of mean concentrations in the three experimental groups, the mean fold change was calculated as the ratio between the mean concentration of each of the tested doses of cisplatin, and the mean concentration of the saline group. The fold changes were transformed to a log2 scale to accommodate the dynamic range in the concentration values.[22]

2.6 | Assessment of the Kidney/Body Mass Index

The body weight of the animals of the different experimental groups were measured after anesthesia. After euthanasia, the kidneys were surgically removed and weighed. The kidney/body mass index was calculated as follows: kidney weight/body weight.

2.7 | Western blot analysis

After treatment, heart left ventricle, aorta and renal tissue were dissected and frozen immediately at −80°C. The samples were obtained from 5–6 animals per experimental group.

For protein extraction in cardiac and renal tissues, they were homogenized with ice-cold RIPA buffer containing 1 mM EGTA, 1 Mm Na_3VO_4, 1 mM $Na_4P_2O_7$, 10 mM NaF, and a protease inhibitor cocktail (Roche, Spain). For protein extraction of aorta tissues,

the vessel was frozen with liquid nitrogen and homogenized, the fragments were suspended and agitated in RIPA buffer, later the sampler were placed on ice for 10 min. All homogenates were centrifuged, and the supernatant was extracted. Total protein values were quantified from all preparations using the Bradford method.[16]

To perform the electrophoresis, left ventricle (40 μg), aorta (20 μg or 40 μg), and kidney (40–60 μg) were loaded onto a 4–15 or 10%Mini-Protean® TGX™ Precast Gel (Bio-Rad, Spain) and, then transferred into a PVDF membrane (Bio-Rad, Spain). The membranes were blocked with 3% of non-fat dry milk at room temperature for 1 h and then incubated at 4° overnight with the primary antibodies: TLR4 1:500 (left ventricle), 1:2000 (aorta), 1:1000 (kidney) (Novus Biosciences Cat#NB100-56566); MyD88 1:500 (left ventricle, kidney), 1:1000 (aorta) (Abcam, Cat#2064); NLRP3 1:750 (left ventricle), 1:1000 (aorta, kidney) (Abcam, Cat#263899); procaspase-1 1:1000 (left ventricle, aorta, kidney) (Abcam, Cat#286195); NF-κβ p65 1:1000 (kidney) (Abcam, Cat#16502). These incubations were followed by incubation for 1 h at room temperature with the specific secondary antibody (goat anti-mouse horseradish peroxidase (HRP))-conjugated secondary antibody (Thermo Fisher Scientific, Inc, Cat#31430) or goat anti-rabbit HRP-conjugated secondary antibody (Thermo Fisher Scientific, Inc, Cat#31460). Glyceraldehyde-3-phosphate dehydrogenase (GAPDH) 1:5000 (Abcam, Cat#8245) was used as a loading control with secondary antibody (1:10000).

The membrane was then incubated with Clarity Western ECL substrate (Bio-Rad, Spain) and protein bands were detected using a Chemidoc XRS+ system. Bands were examined by densitometry using ImageLab software (BioRad, Spain) and normalized to the loading control.

2.8 | Immunohistochemical analysis in mesenteric artery

Since methodological problems did not allow carry out Western Blot analysis in the mesenteric bed, immunohistological studies were conducted.

Firstly, we performed routine hematoxylin–eosin-stained slides: samples of 5 mm3 were fixed in 10% formaldehyde at room temperature, embedded in paraffin and cut into 5-micron-thick slices in a Micron HM360 microtome.

Thereafter, we chose a representative paraffin block from each case and performed immunohistochemistry for TLR4, MyD88 and NLRP3 factors. Histology sections were deparaffinized and rehydrated before endogenous peroxidase activity was blocked with H_2O_2 (0.3%) in methanol. The slides were rinsed with PBS and incubated with primary antibodies in a moist chamber at room temperature. The sections were subsequently incubated with biotinylated anti-rabbit IgG and LBA (DAKO) for 25 min at room temperature, rinsed with PBS and immersed for 25 min in avidin peroxidase. The immunostaining reaction product was developed

using diaminobenzidine. Counterstaining was performed with hematoxylin. The specificity of the immunohistochemical procedure was confirmed by incubation of sections with non-immune serum instead of a primary antibody.

The primary antibodies used were anti-TLR4 antibody (Novusbio, Cat#NB100-56566 1/50), anti-MyD88 antibody (Abcam, Cat#131071, 1/1500), anti- NLRP3 antibody (Invitrogen, Cat#SC06-23, 1/50).

All histological slides were studied under a Zeiss Axiophot 2 microscope and photographed with an Axiocam HRc camera. All the histological slides were evaluated by the same researcher without knowledge of the groupings.

2.9 | Statistical analysis

Data represent mean values ± SEM for at least 4–7 rats. Data were analyzed by one-way analysis of variance (ANOVA). To compare means Tukey post hoc test was used, using the GraphPad Prism 8 software (San Diego, CA). In the histological analysis, the differences between groups were assessed using the corrected chi-squared test. P-values ≤0.05 were considered significant.

2.10 | Compounds and drugs

Cisplatin was obtained from Sigma (Sigma Chemical Company, Poole, Dorset, UK) and dissolved in saline (0.9% NaCl).

2.11 | Nomenclature of targets and ligands

Key protein targets and ligands in this article are hyperlinked to corresponding entries in http://www.guidetopharmacology.org, the common portal for data from the IUPHAR/BPS Guide to PHARMACOLOGY,[23] and are permanently archived in the Concise Guide to PHARMACOLOGY 2019/20.[24]

3 | RESULTS

3.1 | Effects of cycles cisplatin treatment on production of oxidative damage

Cisplatin cycles administration caused an increase in MDA level at the two doses evaluated (cisplatin 2 mg/kg: 0.286 ± 0.047 mMol/mL, $n = 5$ $p > .05$); cisplatin 3 mg/kg-treated group (0.559 ± 0.116 mMol MDA/mL, $n = 4$, $p < .05$ vs. saline group: 0.242 ± 0.023 mMol/mL, $n = 4$). Moreover, the increase in MDA level was dose-dependent, being significantly higher with cisplatin 3 mg/kg than with cisplatin 2 mg/kg cycles treatment (cisplatin 2 mg/kg: 0.286 ± 0.047 mMol/mL, $n = 5$ vs. cisplatin 3 mg/Kg: 0.559 ± 0.116 mMol MDA/mL, $n = 4$, $p < .05$) (Figure 1).
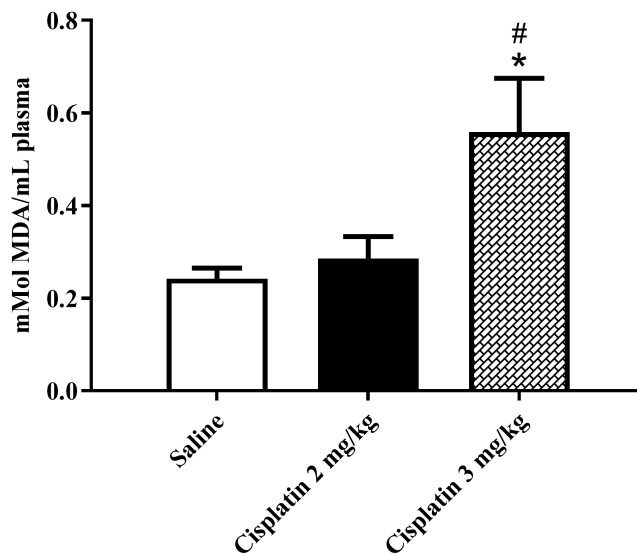

FIGURE 1 Effect of cisplatin cycles administration on malondialdehyde (MDA) plasma concentrations at the end of the study in the different groups. Each bar represents Mean ± SEM of 4–5 samples from 4–5 animals per experimental group. A one-way analysis of variance (ANOVA) followed by Tukey post hoc test was used for statistical (*$p < .05$, cisplatin 3 mg/kg vs. saline, #$p < .05$, cisplatin 2 mg/kg vs. cisplatin 3 mg/kg).

3.2 | Effects of cycles cisplatin treatment on production of cytokines

Plasma levels of different cytokines and chemokines were determined in the different experimental groups (Table 1). No measurable detection in plasma tissue includes VEGF, and IL-2, IL-5, IL-17.

The cisplatin treated animals showed similar values that control animals in the most cytokines and chemokines analyzed (Table 1). However, the animals treated with cycles of cisplatin showed increases in plasma levels of IL-18 in comparison with saline-treated animals (cisplatin 2 mg/kg: 585 ± 88 pg/mL, $n = 4$, $p > .05$; cisplatin 3 mg/kg: 4915 ± 1531 pg/mL, $n = 5$, $p < .05$ vs. saline: 353 ± 69 pg/mL, $n = 5$). Besides, the resulting increase in plasma levels of IL-18 in cisplatin-treated animals was dose-dependent (cisplatin 2 mg/kg: 585 ± 88 pg/mL, $n = 4$, $p < .05$ vs. cisplatin 3 mg/kg: 4915 ± 1531 pg/mL, $n = 5$) (Figure 2).

To analyze, the results obtained in the levels of cytokines and chemokines in which no differences had been found between the experimental groups, a heat map was carried out (Figure 3).

An analysis of trends in this heat map shows that in cisplatin 2 mg/kg group, G-CSF, (GM-CSF), IL-1α, IL-6, TNF-α, IL-12p70, and IL-13 tend to decrease in relation to levels observed in control group, being this decrease greater in the levels of IL-12p70 than in the rest of the cytokines analyzed. No differences were observed in the levels of other cytokines such as IL-4, IL-7, IL-10, IFN-γ, MIP-1α, RANTES, MIP-3α, and GRO/KC between in the cisplatin 2 mg/kg group and the control group. It should also be noted that MCP-1 and IL-1β levels tend to increase in the cisplatin 2 mg/kg group in relation to the control group (Figure 3).

TABLE 1 Overview of plasma cytokines and chemokines levels using bioplex assay in the three experimental groups.

Analyte	Saline	Cisplatin 2 mg/kg	Cisplatin 3 mg/kg	p-value
G-CSF	56.68 ± 4.51	47.94 ± 9.56	51.67 ± 3.96	ns
(GM)-CSF	85.17 ± 8.74	65.59 ± 13.47	90.58 ± 13.25	ns
IL-1α	118.9 ± 12.77	87.87 ± 23.55	94.88 ± 7.89	ns
IL-1β	28.36 ± 2.77	41.27 ± 9.23	28.50 ± 2.34	ns
IL-6	209.09 ± 38.14	180.81 ± 32.84	189.79 ± 17.55	ns
TNF-α	353.50 ± 53.19	299.51 ± 53.77	314.93 ± 41.38	ns
IL-4	89.77 ± 19.93	98.95 ± 23.13	85.73 ± 14.46	ns
IL-7	70.59 ± 9.30	72.74 ± 19.91	62.84 ± 7.42	ns
IL-10	214.24 ± 17.11	234.74 ± 57.21	194.80 ± 34.51	ns
IL-12p70	191.22 ± 54.67	154.74 ± 57.15	147.13 ± 15.49	ns
IL-13	89.65 ± 16.72	82.31 ± 21.12	87.46 ± 15.31	ns
IL-18	**353.03 ± 68.98**	**584.87 ± 87.80**	**4915.55 ± 1530.61**[**, #]	**, #
IFN-γ	173.74 ± 28.81	194.47 ± 43.72	199.39 ± 22.38	ns
MCP-1	22195.03 ± 2163.59	27221.42 ± 4797.82	25477.21 ± 1171.22	ns
MIP-1α	44.72 ± 1.66	43.33 ± 7.67	50.53 ± 5.82	ns
RANTES	11351.34 ± 885.93	11770.11 ± 1752.60	13435.66 ± 1337.12	ns
MIP-3α	1406.02 ± 113.10	1413.67 ± 112.73	1297.01 ± 16.45	ns
GRO/KC	278.85 ± 41.11	309.26 ± 98.84	233.97 ± 26.24	ns

Note: Data are presented as Mean ± SEM of observations obtained for 4–6 tissues samples from 4–6 animals per treatment. A one-way ANOVA followed by Tukey post hoc test was used for statistical analysis (ns: not significant, **$p < .01$, cisplatin 3 mg/kg vs. saline, #$p < .05$ cisplatin 3 mg/kg vs. cisplatin 2 mg/kg).
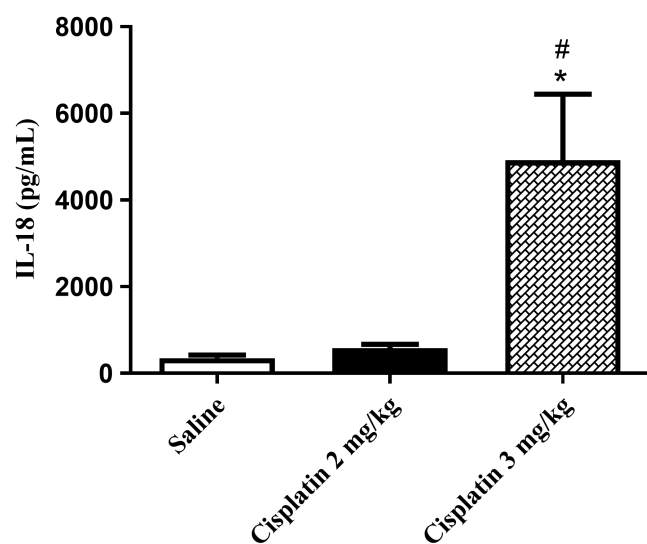

FIGURE 2 Effect of cisplatin cycles administration on the levels of systemic IL-18 plasma levels at the end of the study in different groups. Each bar represents Mean ± SEM of 4–5 samples from 4–5 animals per experimental group. A one-way analysis of variance (ANOVA) followed by Tukey post hoc test was used for statistical (*$p < .05$, cisplatin 3 mg/kg vs. saline, #$p < .05$, cisplatin 2 mg/kg vs. cisplatin 3 mg/kg).

In cisplatin 3 mg/kg group the tendency to decrease was observed in the IL-1α, TNF-α, IL-7, IL-10, GRO-KC, and IL-12p70, again being the greatest decrease in the case of IL-12p70. No differences were observed in the levels of other cytokines such as G-CSF, (GM)-CSF, IL-1β, IL-6, IL-4, IL-13, IFN-γ, MCP-1, MIP-1α, MIP-3α. It should also be noted that RANTES levels tend to increase in the cisplatin 3 mg/kg group in relation to the control group (Figure 3).

3.3 | Effects of cycles cisplatin treatment on the expression of TLR4, MyD88, NLRP3, procaspase-1, and cleaved-caspase-1 in left ventricle tissue

The cycles treatment with cisplatin 2 mg/kg and 3 mg/kg did not modify the expression of TLR4 (cisplatin 2: 106.86 ± 6.66 U.A, $n = 6$, $p > .05$; cisplatin 3: 100.41 ± 5.53 U.A, $n = 6$, $p > .05$ vs. saline: 100.00 ± 5.66 U.A, $n = 6$), and the expression of MyD88 (cisplatin 2: 97.99 ± 5.58 U.A, $n = 5$, $p > .05$; cisplatin 3: 101.99 ± 7.91 U.A, $n = 6$, $p > .05$ vs. saline: 100.00 ± 2.19 U.A, $n = 4$) in the left cardiac ventricle in relation with saline treatment (Figure 4A,B).

However, this antitumoral treatment caused an increase in the expression of NLRP3 in cardiac tissue (cisplatin 2 mg/kg: 234.98 ± 25.53 U.A, $n = 6$, $p > .05$; cisplatin 3 mg/kg: 565.68 ± 154.63 U.A, $n = 5$, $p < .01$ vs. saline: 100.12 ± 8.80 U.A, $n = 6$) (Figure 5A). Moreover, the increase in the expression of NLRP3 was dose-dependent (cisplatin 3 mg/kg: 565.68 ± 154.63 U.A, $n = 5$, $p < .05$ vs. cisplatin 2 mg/kg: 234.98 ± 25.53 U.A, $n = 6$) (Figure 5A).

To confirm the implication of NLRP3 pathway in the cardiac damage caused, the expressions of procaspase-1 and cleaved-caspase-1 were
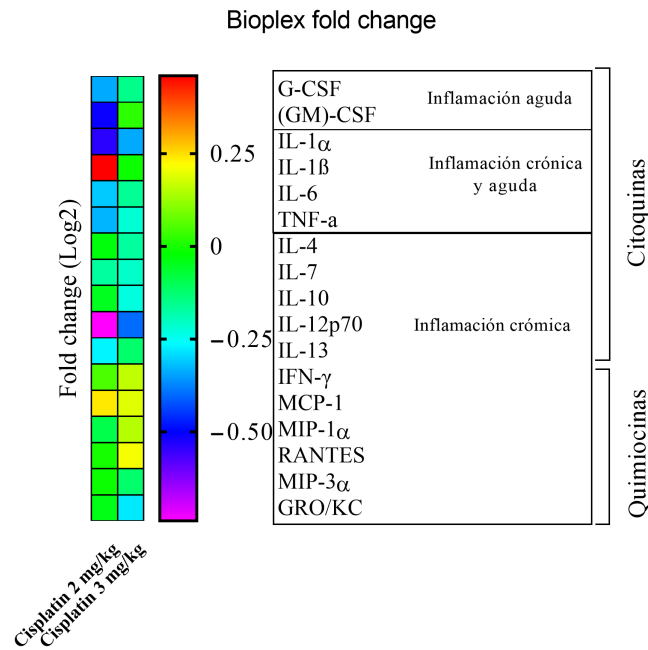
Bioplex fold change

FIGURE 3 Visualization of the intergroup differences (cisplatin 2 mg/kg, cisplatin 3 mg/kg) of non-significative cytokines and chemokines measured by Bio-Plex Pro™ Rat Cytokine in plasma, using a heatmap. Data are presented as the ratio of presented as the log2 of the ratio of the mean of the groups treated with cisplatin with the mean of the saline group, respectively. Red light indicates elevated levels, green light indicates same levels, blue and purple levels indicate low levels. G-CSF (granulocyte colony-stimulating factor), (GM)-CSF (granulocyte-macrophage colony-stimulating factor), IL-1α, IL-1β, IL-6, TNF-α (tumor necrosis factor-α), IL-4, IL-7, IL-10, IL-12p70, IL-13, IFN-γ (interferon γ), MCP-1 (monocyte chemoattractant protein-1), MIP-1α (macrophage inflammatory protein 1 α), RANTES (C-C motif chemokine ligand 5), MIP-3α (macrophage inflammatory protein 3 α), GRO/KC (chemokine (C-X-C motif) ligand 1).

analyzed. The chronic treatment with cisplatin 2 mg/kg did not modify the expression of procaspase-1, and cleaved-caspase-1 in left ventricle tissue (procaspase-1: cisplatin 2 mg/kg: 96.33 ± 8.04 U.A, $n=5$, $p>.05$; vs. saline: 100.00 ± 4.10 U.A, $n=5$; cleaved-caspase-1: cisplatin 2 mg/kg: 96.98 ± 4.47 U.A, $p>.05$ vs. saline: 100.00 ± 3.69 U.A, $n=5$) (Figure 5B,C). However, chronic treatment with cisplatin 3 mg/kg caused a, slight although not significant, increase in the expression of pro-caspase-1, and cleaved-caspase-1 in this tissue (procaspase-1: cisplatin 3 mg/kg: 111.81 ± 6.39 U.A, $n=5$, $p>.05$ vs. saline: 100.00 ± 4.10 U.A, $n=5$; cleaved-caspase-1: cisplatin 3 mg/kg: 111.93 ± 11.27 U.A, $n=5$, $p>.05$ vs. saline: 100.00 ± 3.69 U.A, $n=5$) (Figure 5B,C).

3.4 | Effects of cycles cisplatin treatment on expression of TLR4, MyD88, NLRP3, procaspase-1, and cleaved-caspase-1 in aorta

The cycles treatment with cisplatin 2 mg/kg, and 3 mg/kg did not modify the expression of TLR4 (cisplatin 2: 97.64 ± 8.32 U.A, $n=6$, $p>.05$; cisplatin 3: 97.36 ± 9.88 U.A, $n=5$, $p>.05$ vs. saline:

100.00 ± 3.50 U.A, $n=6$), and the expression of MyD88 (cisplatin 2: 97.99 ± 5.58 U.A, $n=5$, $p>.05$; cisplatin 3: 101.99 ± 7.91 U.A, $n=6$, $p>.05$ vs. saline: 100.00 ± 2.19 U.A, $n=4$) in aortic tissue in relation with saline treatment (Figure 6A,B).

However, the cycles treatment with cisplatin provoked a significant decrease in the expression of NLRP3 in this vascular tissue in comparison with saline treatment (cisplatin 2 mg/kg: 75.08 ± 6.90 U.A, $n=6$, $p<.05$; cisplatin 3 mg/kg: 58.64 ± 3.83 U.A, $n=6$, $p<.01$ vs. saline: 100.00 ± 8.19 U.A, $n=7$). Moreover, the decrease in the expression of NLRP3 seems to be dose-dependent since it was higher with chronic treatment with cisplatin 3 mg/kg than with cisplatin 2 mg/kg (cisplatin 3 mg/kg: 58.64 ± 3.83 U.A, $n=6$, $p>.05$; cisplatin 2 mg/kg: 75.08 ± 6.90 U.A, $n=6$) (Figure 7A).

To confirm the results obtained in the expression of NLRP3 pathway in aorta, the expression of procaspase-1 and cleaved-caspase-1 was analyzed in treated groups. The cycles treatment with cisplatin 2 mg/kg caused a sight, but not significant, decrease in the expression of procaspase-1 in aorta in relation with saline treatment (cisplatin 2 mg/kg: 83.31 ± 11.53 U.A, $n=5$, $p>.05$ vs. saline: 100.00 ± 5.23 U.A, $n=5$). Besides, treatment with cycles of cisplatin 3 mg/kg produced a significant decrease in the expression of procaspase-1 (cisplatin 3 mg/kg: 61.98 ± 11.46 U.A, $n=5$, $p<.05$ vs. saline: 100.00 ± 5.23 U.A, $n=5$) (Figure 7B). In parallel, the cycles treatment with cisplatin 2 mg/kg and 3 mg/kg caused a significant decrease in the expression of cleaved-caspase-1 (cisplatin 2 mg/kg: 46.51 ± 9.45 U.A, $n=4$, $p<.05$; cisplatin 3 mg/kg: 29.19 ± 13.45 U.A, $n=5$, $p<.001$ vs. saline: 100.00 ± 5.50 U.A, $n=5$) (Figure 7C).

3.5 | Effects of cycles cisplatin treatment on expression of TLR4, MyD88, and NLRP3 in mesenteric artery

In the mesenteric artery, the changes produced by cisplatin cycles treatment in the expression of TLR4, MyD88 and NLRP3 have been analyzed in the three tissue layers: endothelium (intima layer), muscular smooth muscle cells (middle layer) and adventitia (outer layer).

In endothelium and middle layer, cycles treatment with cisplatin 2 mg/kg and 3 mg/kg caused an increase in the expression of TLR4 and MyD88, that resulted higher at the maximum dose administered. The expression of NLRP3 was not modified at the endothelium and middle layer after chronic treatment with cisplatin 2 mg/kg and 3 mg/kg (Figure 8).

In adventitia layer, chronic treatments with cisplatin 2 mg/kg and 3 mg/kg did not cause changes in the expression of TLR4, MyD88, and NLRP3 (Figure 8).

3.6 | Effects of cycles cisplatin treatment on changes in Kidney/Body Mass Index

The cycles cisplatin treatments caused a dose-dependent significant decrease in body weight (cisplatin 2 mg/kg: 296.00 ± 13.88 g, $n=6$,
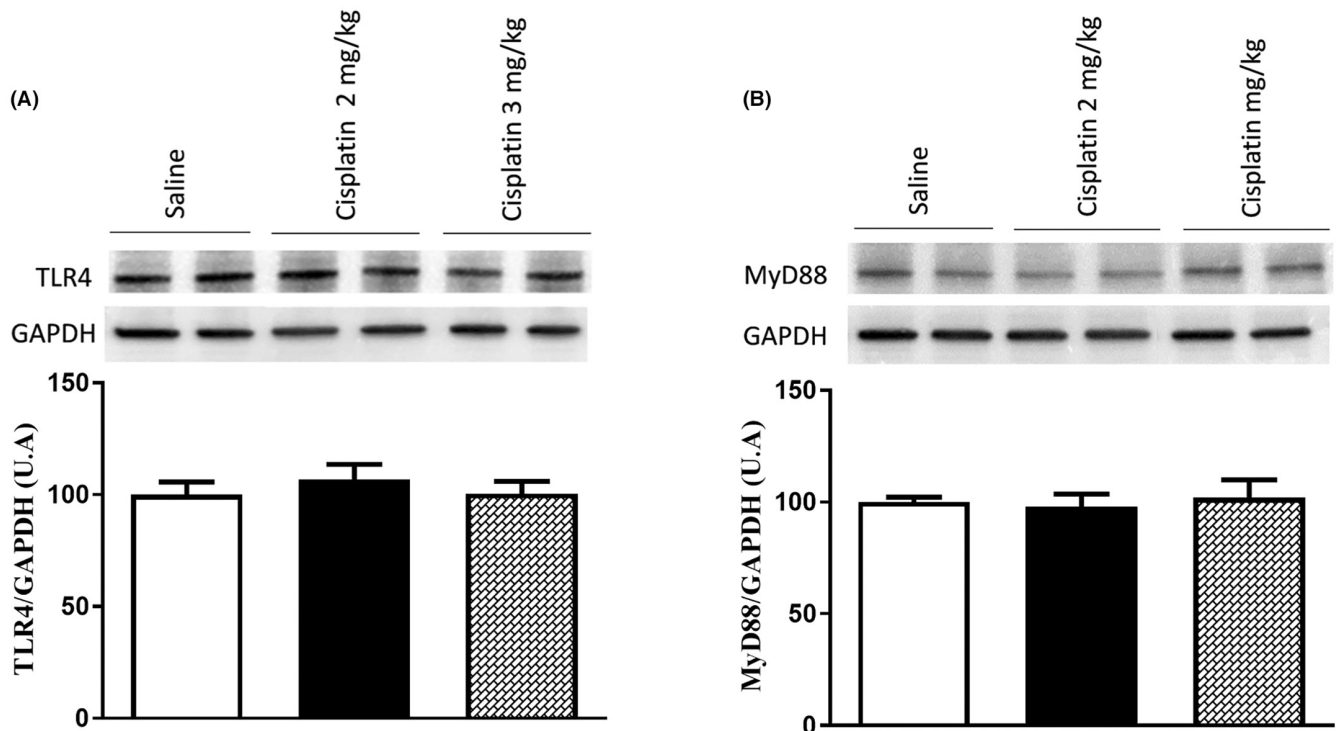
FIGURE 4 Representative immunoblots for TLR4 (A), and MyD88 (B) protein expression in whole cardiac left ventricle. Diagram bars show the results of densitometric analysis in whole cardiac left ventricle. Data are presented as Mean±SEM of observations obtained for 4–6 tissues samples from 4–6 animals per treatment. A one-way analysis of variance (ANOVA) followed by Tukey post hoc test was used for statistical.
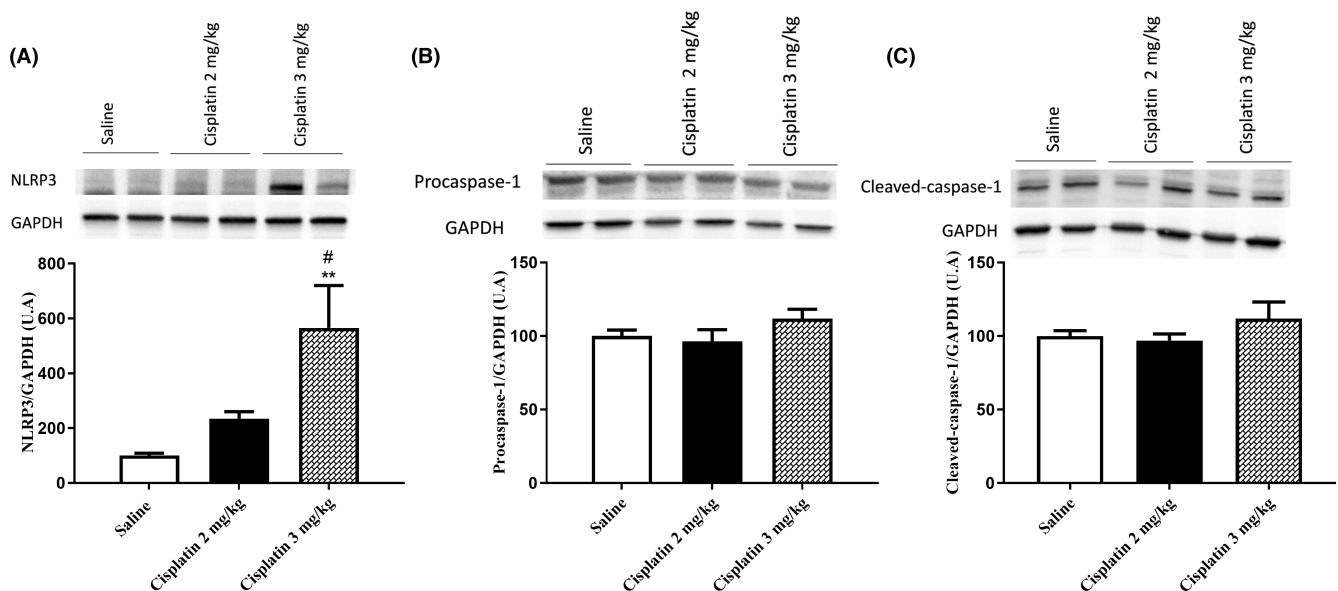

FIGURE 5 Representative immunoblots for NLRP3 (A), procaspase-1 (B), and cleaved-caspase-1 (C) protein expression in whole cardiac left ventricle. Diagram bars show the results of densitometric analysis in whole cardiac left ventricle. Data are presented as Mean±SEM of observations obtained for 5–6 tissues samples from 5–6 animals per treatment. A one-way analysis of variance (ANOVA) followed by Tukey post hoc test was used for statistical (**$p < .01$ cisplatin 3 mg/kg vs. saline, #$p < .05$ cisplatin 3 mg/kg vs. cisplatin 2 mg/kg).

$p < .001$; cisplatin 3 mg/kg: 230.28 ± 8.78 g, $n = 7$, $p < .0001$ vs. saline: 380.33 ± 10.17 g, $n = 6$). Contrary, a dose-dependent increase in kidney mass was observed after cycles cisplatin treatment (cisplatin

2 mg/kg: 1.43 ± 0.21 g, $n = 6$, $p > .05$; cisplatin 3 mg/kg: 2.52 ± 0.28 g, $n = 7$, $p < .001$ vs. saline: 1.14 ± 0.03 g, $n = 6$). So, cisplatin chronic treatment provoked a dose-dependent increase in kidney/body mass
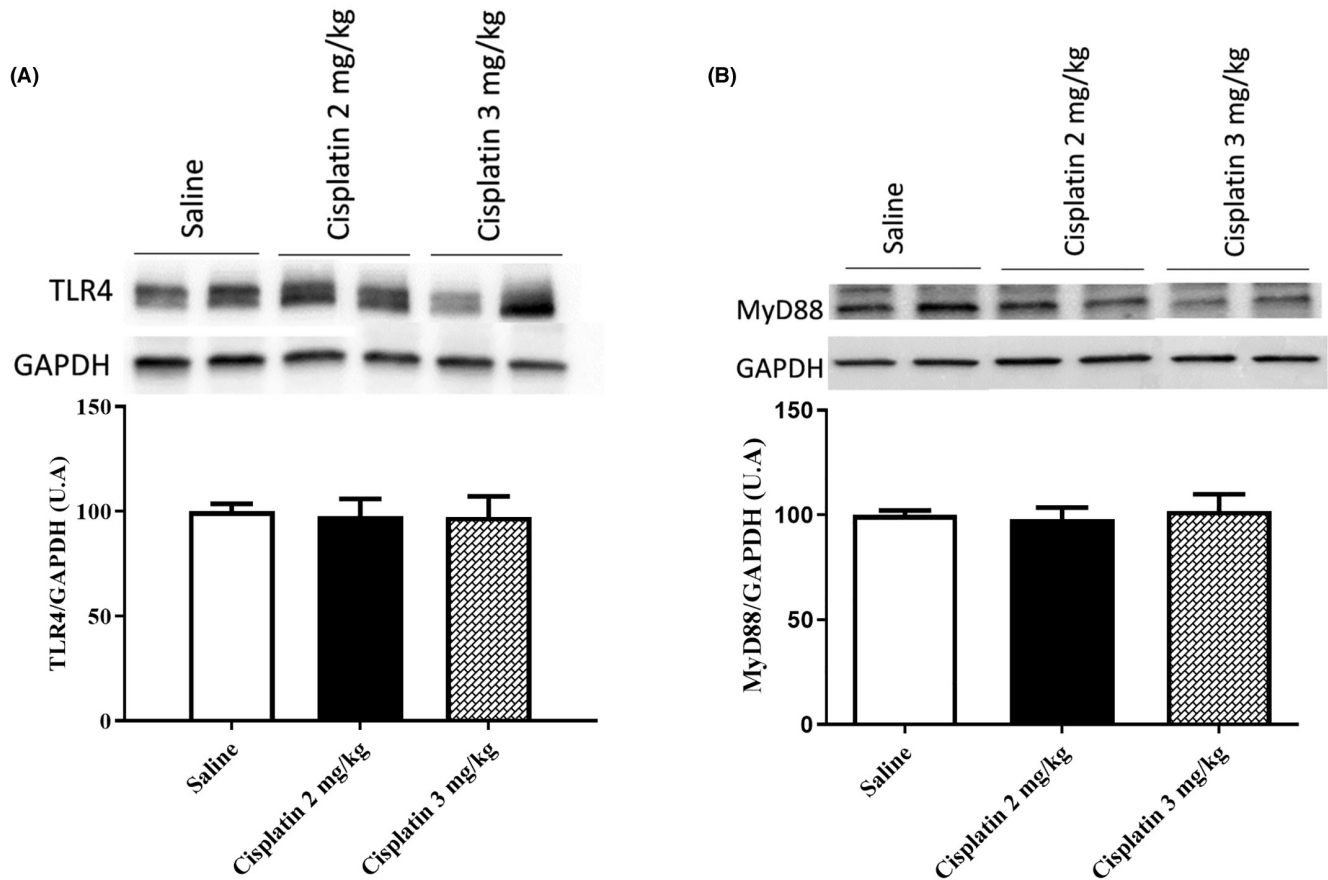
FIGURE 6 Representative immunoblots for TLR4 (A), and MyD88 (B) protein expression in aorta. Diagram bars show the results of densitometric analysis in aorta. Data are presented as Mean $\pm$ SEM of observations obtained for 4–6 tissues samples from 4–6 animals per treatment. A one-way analysis of variance (ANOVA) followed by Tukey post hoc test was used for statistical.

FIGURE 7 Representative immunoblots for NLRP3 (A), procaspase-1 (B), and cleaved-caspase-1 (C) protein expression in aorta. Diagram bars show the results of densitometric analysis in aorta. Data are presented as Mean $\pm$ SEM of observations obtained for 4–6 tissues samples from 4–6 animals per treatment. A one-way analysis of variance (ANO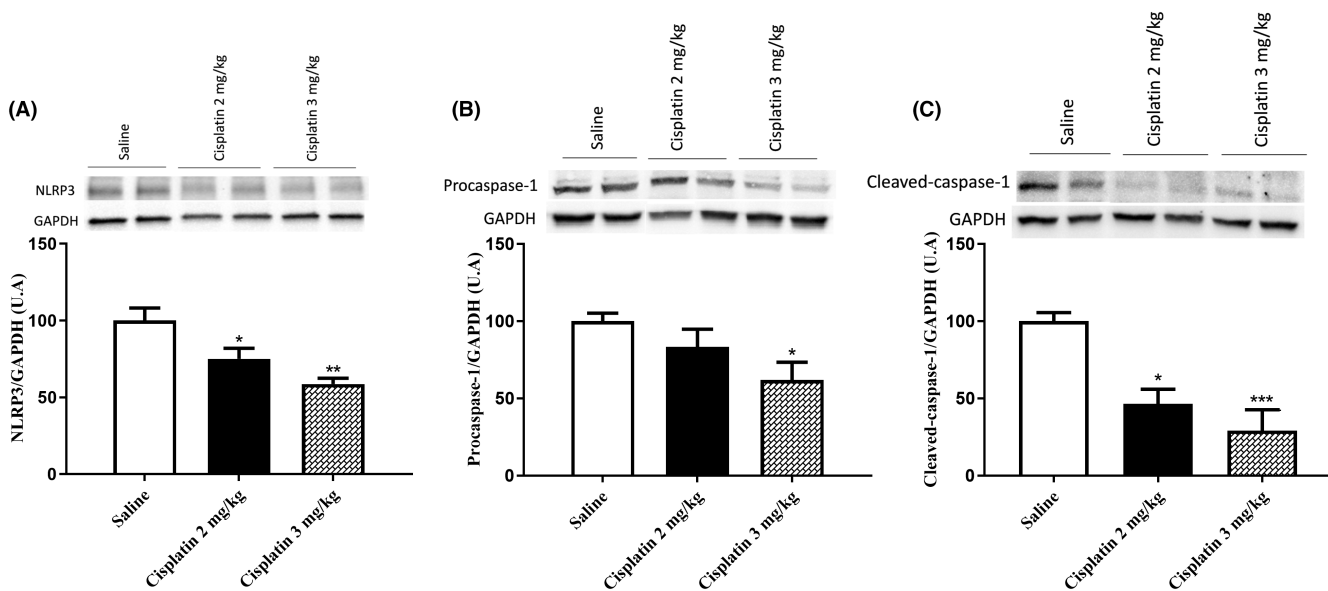VA) followed by Tukey post hoc test was used for statistical ($***p < .001$ cisplatin 3 mg/kg vs. saline, $**p < .01$ cisplatin 3 mg/kg vs. saline, $*p < .05$, cisplatin 3 mg/kg vs. saline).
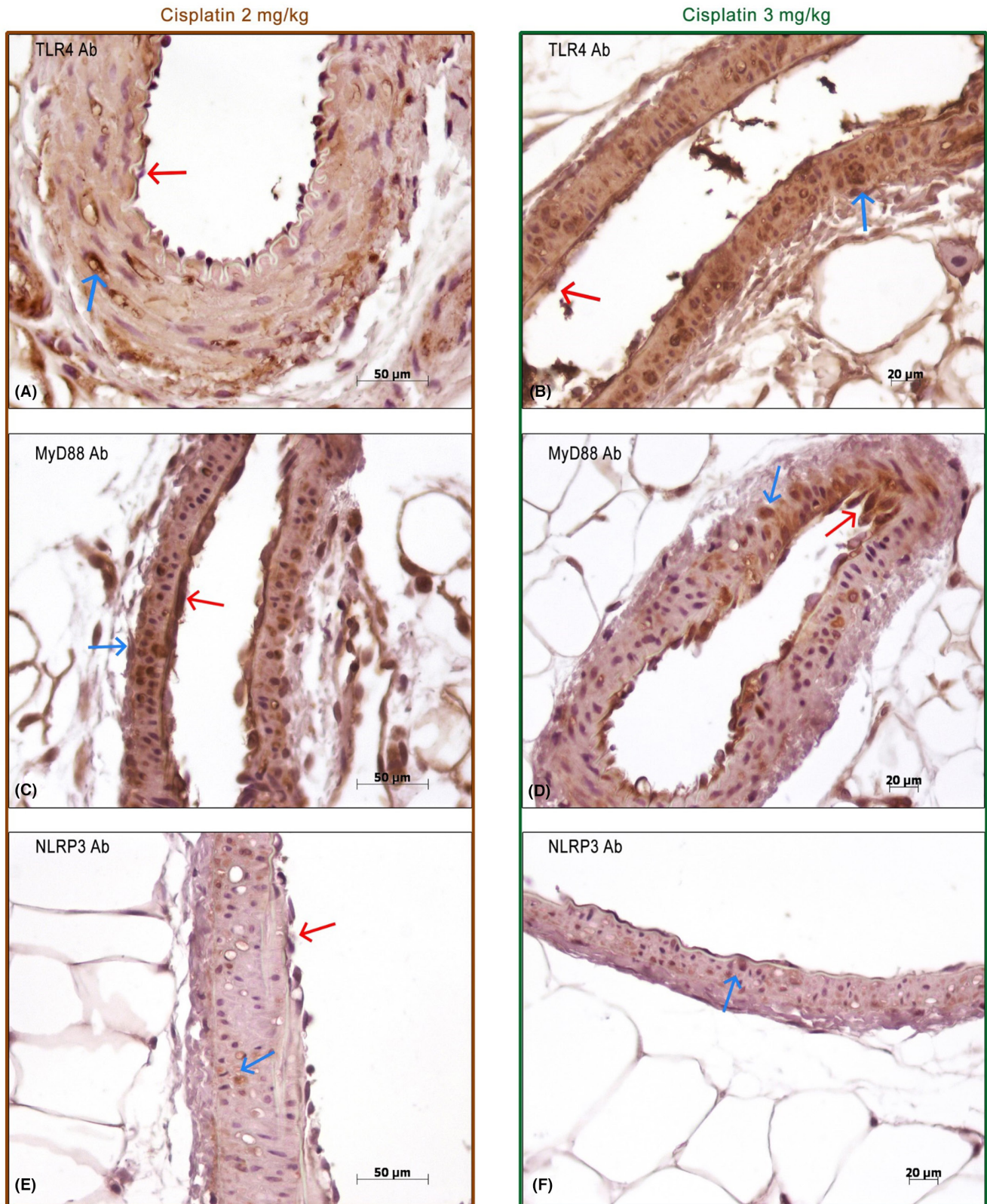
FIGURE 8 Representative images of immunohistochemistry (400×) of the mesenteric artery principal branches, after of cisplatin cycles administration. TLR4 expression in endothelial cells (red arrow) and smooth muscle cells (blue arrow) in cisplatin 2 mg/kg (A), and cisplatin 3 mg/kg (B) groups. MyD88 expression in endothelial cells (red arrow) and smooth muscle cells (blue arrow) in cisplatin 2 mg/kg (C), and cisplatin 3 mg/kg (D) groups. NLRP3 expression in endothelial cells (red arrow) and smooth muscle cells (blue arrow) in cisplatin 2 mg/kg (E), and cisplatin 3 mg/kg (F) groups.

index that was significant at maximum cisplatin dose administered (cisplatin 2mg/kg: 0.005 ± 0.001 g, $n = 6$, $p > .05$; cisplatin 3mg/kg: 0.011 ± 0.001 g, $n = 7$, $p < .0001$ vs. saline: 0.003 ± 0.000, $n = 6$). (Figure 9).

3.7 | Effects of cycles cisplatin treatment on expression of TLR4, MyD88, NLRP3, NF-κβ p65, procaspase-1, and cleaved-caspase-1, in kidney

The cycles treatment with cisplatin caused an increase in the expression of TLR4 at the two doses evaluated in renal tissue in comparison with saline treatment (cisplatin 2mg/kg: 173.77 ± 18.18 U.A, $n = 6$, $p > .05$; cisplatin 3mg/kg: 379.74 ± 64.82 U.A, $n = 5$, $p < .001$ vs. saline: 100.00 ± 2.06 U.A, $n = 6$). Besides, this antitumoral treatments provoked a significant increase in the expression of MyD88 in renal tissue in comparison with saline treatment. (cisplatin 2mg/kg: 232.03 ± 36.62 U.A, $n = 5$, $p < .05$; 342.72 ± 35.63 U.A, $n = 5$, $p < .0001$ vs. saline: 100.00 ± 1.40 U.A, $n = 6$). Moreover, the increase in the expression of TLR4 and MyD88 in renal tissue was dose-dependent (TLR4 cisplatin 3mg/kg: 379.74 ± 64.82 U.A, $n = 5$, $p < .01$ vs. TLR4 cisplatin 2mg/kg: 173.77 ± 18.18 U.A, $n = 6$; MyD88 cisplatin 3mg/kg: 342.72 ± 35.63 U.A, $n = 5$, $p < .05$ vs. MyD88 cisplatin 2mg/kg: 232.03 ± 36.62 U.A, $n = 5$) (Figure 10A,B).

To confirm the involvement of TLR4 and MyD88 in kidney damage, the expression of NF-κβ p65 was analyzed. The cycles treatment with cisplatin 2mg/kg did not cause any change in the expression of NF-κβ p65 in renal tissue in comparison with saline treatment (cisplatin 2mg/kg: 77.37 ± 7.10 U.A, $n = 6$, $p > .05$ vs. saline: 100.00 ± 2.78 U.A, $n = 5$). However, cycles treatment

with cisplatin 3mg/kg caused a significant increase in the expression of NF-κβ p65 in renal tissue in comparison with saline treatment (cisplatin 3mg/kg: 193.27 ± 28.86 U.A, $n = 5$, $p < .01$ vs. saline: 100.00 ± 2.78 U.A, $n = 5$) (Figure 10C) and 2mg/kg cycles of cisplatin (cisplatin 3mg/kg: 193.27 ± 28.86 U.A, $n = 5$, $p < .001$ vs cisplatin 2mg/kg: 77.37 ± 7.10 U.A, $n = 6$).

The cycles treatment with cisplatin 2mg/kg and 3mg/kg caused a significant increase in the expression of NLRP3 (cisplatin 2mg/kg: 864.40 ± 167.53 U.A, $n = 6$, $p < .01$; cisplatin 3mg/kg: 1664.93 ± 142.72 U.A, $n = 6$, $p < .0001$ vs. saline: 100.02 ± 4.53 U.A, $n = 6$) in relation with saline treatment (Figure 11A). Moreover, the resulting increase in the expression of NLRP3 in renal tissue was also dose-dependent (NLRP3 cisplatin 3mg/kg: 1664.93 ± 142.77 U.A, $n = 6$, $p < .01$ vs. NLRP3 cisplatin 2mg/kg: 864.40 ± 167.53 U.A, $n = 6$) (Figure 11A).

To confirm the involvement of NLRP3 pathway in kidney damage observed, the expression of procaspase-1, and cleaved-caspase-1 was analyzed. The cycles treatment with cisplatin 2mg/kg and cisplatin 3mg/kg caused a slight but not significant increase in the expression of procaspase-1 (cisplatin 2mg/kg: 138.27 ± 13.39 U.A, $n = 5$, $p > .05$; cisplatin 3mg/kg: 138.92 ± 15.91 U.A, $n = 5$, $p > .05$ vs. saline: 100.00 ± 5.49 U.A, $n = 4$) in relation with saline treatment (Figure 11B). With regard to of the expression of cleaved-caspase-1, the cycles treatment with cisplatin 2mg/kg caused a dose-dependent increase in renal tissue (cisplatin 2mg/kg: 138.12 ± 34.21 U.A, $n = 5$, $p > .05$; cisplatin 3mg/kg: 253.84 ± 46.08 U.A, $n = 5$, $p < .01$ vs. saline: 100.00 ± 8.08 U.A, $n = 5$) in relation with saline treatment (Figure 11C).

4 | DISCUSSION

This experimental study demonstrates that cycles treatment of cisplatin causes low-grade systemic inflammation with an early increase in plasma levels of IL-18. Cisplatin proinflammatory state leads to changes in the expression of TLR4, MyD88, or NLRP3 in cardiovascular and renal tissues, being involved in cardio-renal toxicity in cisplatin cycles treatment. The inflammatory sensitivity to tissue damage is earlier at the renal level than at the cardiovascular level. In addition, at the cardiovascular system, resistance vessels are more sensitive than cardiac tissue, and large vessels such as the aorta. TLR4 and NLRP3 are key pathways involved in renal toxicity, while NLRP3 pathway is in cardiac alterations and TLR4 pathway in resistance vessel toxicity. This work is the first to demonstrate the involvement of the TLR4-NLRP3 axis as a common mechanism involved in maintenance renal and cardiovascular damage in cycles therapy with cisplatin.

Clinical data show that cisplatin provokes renal and cardiovascular toxicities that limit its use as antitumor drug.[5,7,25-31] Most of the experimental studies analyze renal and/or cardiovascular toxicity of cisplatin after acute administrations[26,32-34] not in cycles, which is the usual form of administration in the clinical therapy. The experimental model used in this work,[16] mimics the chemotherapy treatment

FIGURE 9 Kidney weight/Body weight ratio in the three experimental groups. Cisplatin cycles administration provoked a dose-dependent increase in kidney/body mass index. Data are expressed as the Mean±SEM from 6–7 animals. A one-way analysis of variance (ANOVA) followed by Tukey post hoc test was used for statistical (****$p < .0001$ cisplatin 3mg/kg vs. saline, ##$p < .01$ cisplatin 3mg/kg vs. cisplatin 2mg/kg).
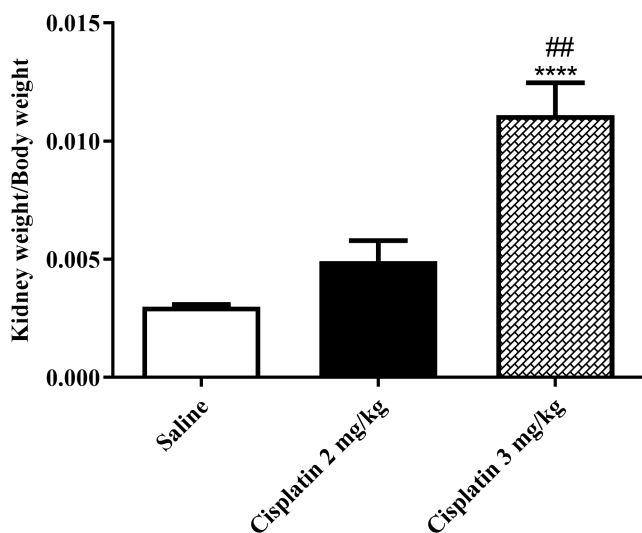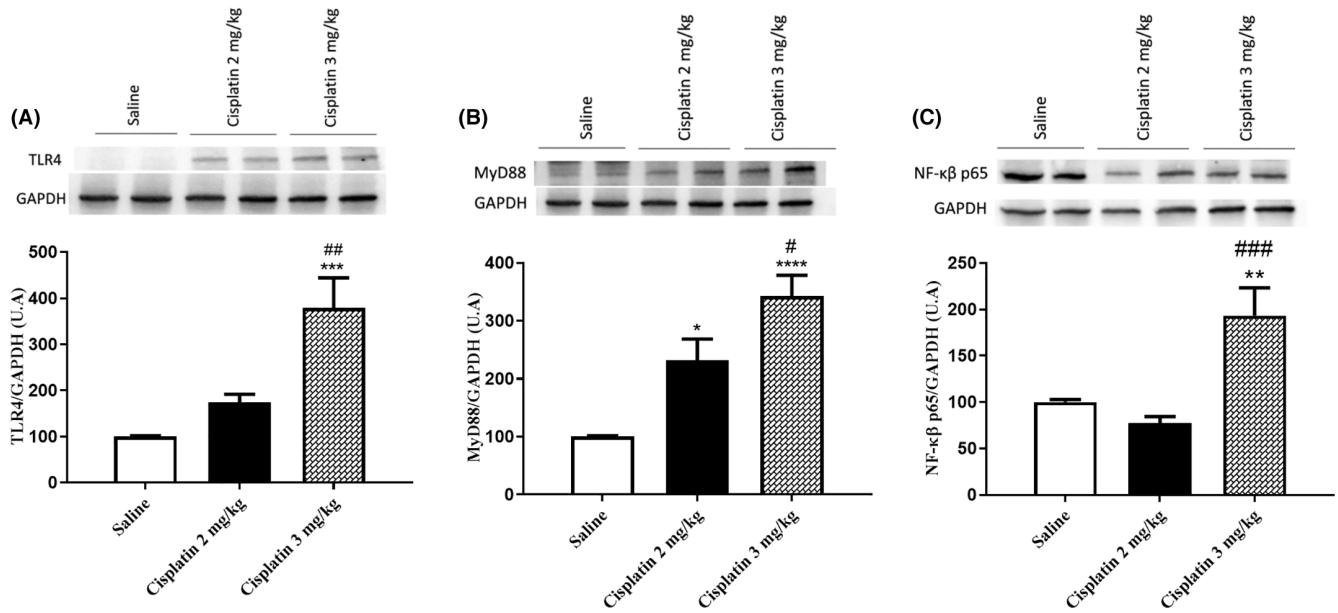
FIGURE 10 Representative immunoblots for TLR4 (A), MyD88 (B), and NF-κβ p65 (C) protein expression in kidney. Diagram bars show the results of densitometric analysis in kidney. Data are presented as Mean±SEM of observations obtained for 5–6 tissues samples from 5–6 animals per treatment. A one-way analysis of variance (ANOVA) followed by Tukey post hoc test was used for statistical (**** $p < .0001$ cisplatin 3 mg/kg vs. saline, *** $p < .001$ cisplatin 3 mg/kg vs. saline, ** $p < .01$ cisplatin 3 mg/kg vs. saline, * $p < .05$ cisplatin 3 mg/kg vs. saline, ### $p < .001$ cisplatin 3 mg/kg vs. cisplatin 2 mg/kg, ## $p < .01$ cisplatin 3 mg/kg vs. cisplatin 2 mg/kg, # $p < .05$ cisplatin 3 mg/kg vs. cisplatin 2 mg/kg).
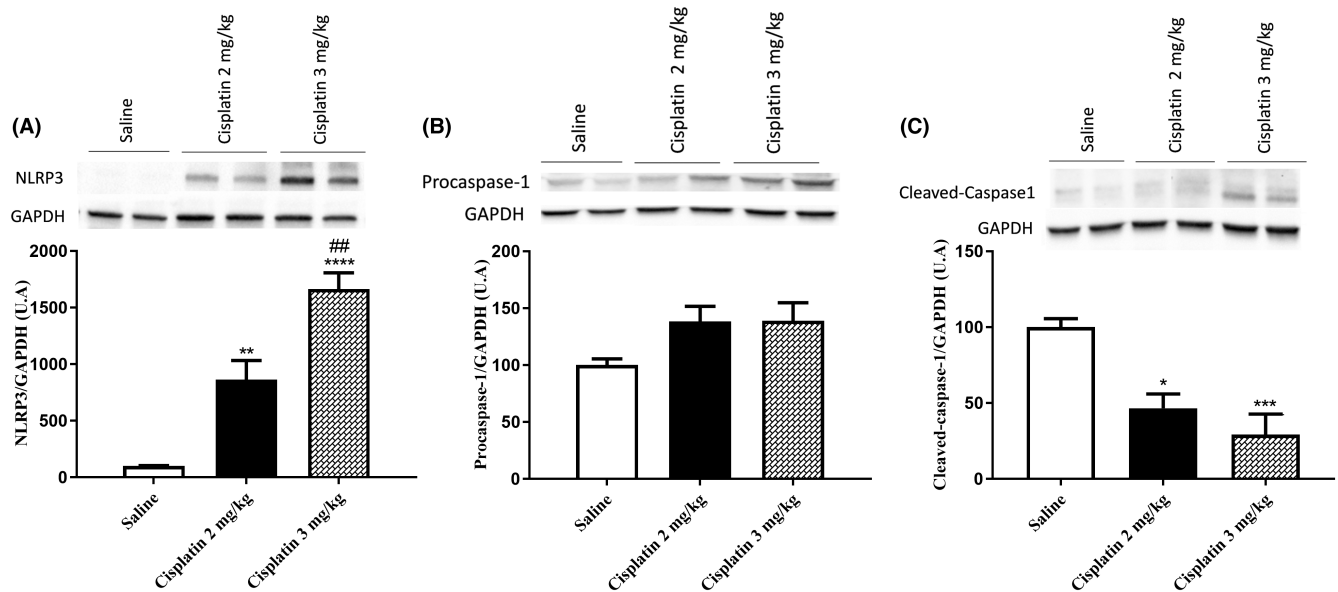

FIGURE 11 Representative immunoblots for NLRP3 (A), procaspase-1 (B), and cleaved-caspase-1 (C) protein expression in kidney. Diagram bars show the results of densitometric analysis in kidney. Data are presented as Mean±SEM of observations obtained for 4–6 tissues samples from 4–6 animals per treatment. A one-way analysis of variance (ANOVA) followed by Tukey post hoc test was used for statistical (**** $p < .0001$ cisplatin 3 mg/kg vs. saline, ** $p < .01$, cisplatin 3 mg/kg vs. saline, ## $p < .001$ cisplatin 3 mg/kg vs. cisplatin 2 mg/kg).

cycles, describing cardiac and vascular alterations with this administration pattern. The present study shows a renal hypertrophy after cisplatin treatments, confirming data described by other authors after single doses,[35–41] or cycles[42] cisplatin treatments. Therefore, the present experimental model would be valid for the study of

mechanisms involved in cardio-renal complications after chronic treatment with cisplatin.

In the present study, a dose-dependent increase in plasma MDA is observed after cycles cisplatin, indicating a generalized oxidative status in the body, as other researchers also described.[2,34,43,44]

It is accepted the involvement of cytokines and chemokines in acute kidney[3,45–47] and cardiovascular toxicity[33,48] produced by cisplatin. However, it is not yet known whether this release of cytokines and chemokines continues after treatment with cisplatin cycles, their role in renal and cardiovascular damage and the sensitivity to this inflammatory state in the different tissues. In the present study, the levels of 23 cytokines and chemokines were analyzed after cycle treatment with cisplatin at two different doses. The results obtained do not show clear patterns of alterations in the proinflammatory mediators. Only a dose-dependent increase in plasma IL-18 levels was observed after treatment with cisplatin. Similar results are described by other authors, proposing IL-18 as critical mediator in acute kidney injury and cardiac damage caused by cisplatin in animal models[47,49–52] and in patients.[53] However, in our study an increase in plasma proinflammatory cytokines such as TNF-α, IL-1β, or IL-6 was not observed after cisplatin treatments. These results have not in accordance with others that describe an increase in these cytokines at the renal and cardiac level after administration of cisplatin.[36,42,54,55] Again, the administration of cisplatin in cycles could causes inflammation at the tissue level prior to generalized inflammation. It is also possible that in our experimental model the acute inflammatory phase has already passed while the development of chronic inflammation is in process.[56–58] Hence, the levels of TNF-α, IL-1β, or IL-6 are no longer so high[56] and a tendency to increase in plasma levels of MCP-1 and RANTES were observed.

Low-grade chronic inflammation contributes to the pathogenesis of toxicity caused by antitumor drugs.[59] In this inflammatory process, toll-like receptor 4 (TLR4) signaling pathway and NOD-like receptor (NLR) family protein (NLRP3) inflammasome play an important role in deleterious organic effects.[60]

Our data demonstrate that TLR4 /MyD88 pathway could maintain the renal damage in cisplatin chronic therapy. The significant increase in the renal expression of NF-κβ p65[36,38,61] after treatment with the maximum dose of cisplatin treatment corroborates the involvement of this pathway. However, more research would be necessary to clarify this aspect, since at the lowest dose of this antitumour used (2 mg/kg), an increase in the expression of TLR4 and MyD88 is observed in this tissue, but no changes in the expression of NF-κβ p65 occur. It is possible that the activation of this mechanism in renal damage depends on the dose of antitumour administered. Our data also show that while the expressions of TLR4 and MyD88 are not increased in cardiac tissue and conduit vessels, they are augmented in mesenteric arteries. Therefore, during treatment with cisplatin cycles, sensitivity to damage seems greater in resistance vessels than at the cardiac level and other vascular territories. These data suggest that renal tissue is much more sensitive to systemic inflammation caused by cisplatin than cardiovascular tissues and that TLR4 pathway is involve in renal damage produced by cyclic antitumoral treatment.

An increase in the tissue expression of NLRP3 is involved in renal injury after acute and chronic cisplatin treatments.[54,62–65] Our data also confirm a dose-dependent increase in the expression of NLRP3 at the renal level. At the cardiovascular system, an increase in the expression of NLRP3 at the cardiac level but not in blood vessels after cisplatin cycles was observed. Other authors also describe similar data in cardiac tissue[52] after treatment with repeated doses cisplatin. Our study is also the first to demonstrate that this increase in NLRP3 expression at the cardiac level is dose-dependent and could maintain cardiotoxicity after cyclic cisplatin treatment.

The canonical activation of the inflammasome is mediated by the formation of a macromolecular complex that involves the three components, NLRP3, ASC and procaspase-1.[66] In all the tissues analyzed in the present study in which expression of NLRP3 is altered, the expression of procaspase-1 and cleaved caspase-1 correlates directly with the expression of NLRP3. This fact confirms that NLRP3 pathway is involve in cardiac and renal damage caused by cisplatin and that the sensitivity to inflammation damage in renal tissue is much more sensitive than cardiac or vascular tissue. In aortic tissue, our results describe a decrease in the expression of NLRP3 that was significant at the highest dose of cisplatin administered, 3 mg/kg. No data have been found in the literature to compare the results obtained in the present study, but this data seem to indicate that the vascular damage caused by the chronic administration of cisplatin is not mediated by the NLRP3 pathway.

Finally, the activation of TLR4 promotes the priming and activation of the NLRP3.[67] The results of our study are partially in agreement with that, since only the activation of the complete TLR4/NLRP3 pathway has been demonstrated in renal tissue. It is possible, that signaling pathways that promote activation of the inflammasome and its components can be different in different tissues.[15]

This experimental work presents different strengths compared to existing studies. First, the experimental model used. It is an animal model that mimics the chemotherapy treatment cycles as clinical treatment is usually done. This model allows not only to assess the acute toxicity of antitumor drugs (after one dose), but also whether this toxicity is maintained throughout the entire antitumor treatment, which is what has been analyzed in this study. Most of the investigations that exist on the toxic effects of cisplatin are carried out after the administration of single doses of the antitumor, not allowing the identification of its possible chronic toxicity. Second, this work analyzes various adverse effects of cisplatin therapy in the same animal. This fact allows to identify whether the toxicity caused by this antitumor appears at the same time and with the same degree of severity in different tissues. In the case of this study, tissues whose functioning is interrelated (cardiovascular and renal) have been analyzed, which is very useful to know if the possible chronic cardiovascular and renal complications caused by cisplatin compensate each other or, if, on the contrary, they enhance each other: Besides, it permits identify common mechanisms in their development to design pharmacological targets for their treatment and/or prevention simultaneously. Third, this work provides information on the mechanisms involved in the cardiac and vascular toxicity of cisplatin that has not been extensively studied up to now, showing for the first time that the activation of NLRP3 is involved in the cardiac damage caused by cisplatin. However, although attempts have been made to analyze the possible relationship of generalized low-grade

inflammation with the cardiovascular and renal toxicity of cisplatin, the results obtained in this study have not been clear, being this fact a weakness in the study. It is possible that the methodology followed, not analyzing the presence of cytokines at the tissue level but at the plasma level, may have led to this lack of conclusive results. On the other hand, the lack of conclusive results on the involvement of the TLR4/MyD88 pathway in the cardiovascular toxicity caused by cisplatin could also be a weakness of the work and that studies with higher doses of cisplatin are necessary to confirm or download the participation of this pathway in the cardiovascular damage caused by this antitumor.

5 | CONCLUSION

In conclusion, this experimental study shows the presence of low-grade systemic inflammation and the participation of TLR4/NLRP3 axis in cardio-renal alterations associated with cycles cisplatin treatment. Besides, it demonstrates that cardiovascular and renal tissues have not the same sensitivity to inflammatory damage caused by cisplatin, being the renal tissue more sensitive than the cardiovascular system. Although more studies are necessary, the present research suggests the interest of modulating the inflammation and the expression of TLR4/NLRP3 for the joint treatment of cardio-renal toxicity during cycles treatment of cisplatin, confirming IL-18 as a systemic marker of low-grade inflammation during treatment with cisplatin.

AUTHOR CONTRIBUTIONS

VL-M designed the study. AG, SGG, FR, EH, and VL-M performed the experiments and analyzed the data. VL-M, EH, and AG wrote the manuscript. All authors reviewed and approved the final version of the manuscript.

CONFLICT OF INTEREST STATEMENT

The authors declare no conflict of interest.

DATA AVAILABILITY STATEMENT

Data are available upon reasonable request.

ORCID

Antonio González https://orcid.org/0000-0001-7689-3704

Visitación López-Miranda https://orcid.org/0000-0003-1378-0387

Esperanza Herradón https://orcid.org/0000-0001-7210-6283

REFERENCES

1. Dasari S, Bernard TP. Cisplatin in cancer therapy: molecular mechanisms of action. *Eur J Pharmacol*. 2014;740:364-378. doi:10.1016/j.ejphar.2014.07.025
2. El-Hawwary AA, Omar NM. The influence of ginger administration on cisplatin-induced cardiotoxicity in rat: light and electron microscopic study. *Acta Histochem*. 2019;121(5):553-562. doi:10.1016/J.ACTHIS.2019.04.013
3. Vasaikar N, Mahajan U, Patil KR, et al. D-pinitol attenuates cisplatin-induced nephrotoxicity in rats: impact on pro-inflammatory cytokines. *Chem Biol Interact*. 2018;290:6-11. doi:10.1016/J.CBI.2018.05.003
4. Ma N, Wei W, Fan X, Ci X. Farrerol attenuates cisplatin-induced nephrotoxicity by inhibiting the reactive oxygen species-mediated oxidation, inflammation, and apoptotic signaling pathways. *Front Physiol*. 2019;10:1419. doi:10.3389/fphys.2019.01419
5. Qian P, Yan LJ, Li YQ, et al. Cyanidin ameliorates cisplatin-induced cardiotoxicity via inhibition of ROS-mediated apoptosis. *Exp Ther Med*. 2018;15(2):1959-1965. doi:10.3892/etm.2017.5617
6. Alexandre J, Moslehi JJ, Bersell KR, Funck-Brentano C, Roden DM, Salem JE. Anticancer drug-induced cardiac rhythm disorders: current knowledge and basic underlying mechanisms. *Pharmacol Ther*. 2018;189:89-103. doi:10.1016/j.pharmthera.2018.04.009
7. Dugbartey GJ, Peppone LJ, De Graaf IAM. An integrative view of cisplatin-induced renal and cardiac toxicities: molecular mechanisms, current treatment challenges and potential protective measures HHS public access. *Toxicology*. 2016;371:58-66. doi:10.1016/j.tox.2016.10.001
8. Yang C, Guo Y, Huang TS, et al. Asiatic acid protects against cisplatin-induced acute kidney injury via anti-apoptosis and anti-inflammation. *Biomed Pharmacother*. 2018;107:1354-1362. doi:10.1016/j.biopha.2018.08.126
9. Qin X, Meghana K, Sowjanya NL, et al. Embelin attenuates cisplatin-induced nephrotoxicity: involving inhibition of oxidative stress and inflammation in addition with activation of Nrf-2/Ho-1 pathway. *Biofactors*. 2019;45(3):471-478. doi:10.1002/biof.1502
10. Huang YC, Tsai MS, Hsieh PC, et al. Galangin ameliorates cisplatin-induced nephrotoxicity by attenuating oxidative stress, inflammation and cell death in mice through inhibition of ERK and NF-kappaB signaling. *Toxicol Appl Pharmacol*. 2017;329:128-139. doi:10.1016/j.taap.2017.05.034
11. Leng B, Tang F, Lu M, Zhang Z, Wang H, Zhang Y. Astragaloside IV improves vascular endothelial dysfunction by inhibiting the TLR4/NF-κB signaling pathway. *Life Sci*. 2018;209:111-121. doi:10.1016/j.lfs.2018.07.053
12. Kim J. Poly(ADP-ribose) polymerase activation induces high mobility group box 1 release from proximal tubular cells during cisplatin nephrotoxicity. *Physiol Res*. 2016;65(2):333-340. Accessed August 26, 2019. http://www.ncbi.nlm.nih.gov/pubmed/26447520
13. Wang Y, Song E, Bai B, Vanhoutte PM. Toll-like receptors mediating vascular malfunction: lessons from receptor subtypes. *Pharmacol Ther*. 2016;158:91-100. doi:10.1016/J.PHARMTHERA.2015.12.005
14. Yu L, Feng Z. The role of toll-like receptor signaling in the progression of heart failure. *Mediators Inflamm*. 2018;2018:1-11. doi:10.1155/2018/9874109
15. Pinar AA, Scott TE, Huuskes BM, Tapia Cáceres FE, Kemp-Harper BK, Samuel CS. Targeting the NLRP3 inflammasome to treat cardiovascular fibrosis. *Pharmacol Ther*. 2020;209:107511. doi:10.1016/j.pharmthera.2020.107511
16. Herradón E, González C, Uranga JA, Abalo R, Martín MI, López-Miranda V. Characterization of cardiovascular alterations induced by different chronic cisplatin treatments. *Front Pharmacol*. 2017;8:196. doi:10.3389/fphar.2017.00196
17. National Research Council (US) Committee for the Update of the Guide for the Care and Use of Laboratory Animals. *Guide for the*

Care and Use of Laboratory Animals. National Academies Press; 2011. doi:10.17226/12910

18. Authier N, Gillet JP, Fialip J, Eschalier A, Coudore F. An animal model of nociceptive peripheral neuropathy following repeated cisplatin injections. *Exp Neurol.* 2003;182(1):12-20. doi:10.1016/S0014-4886(03)00003-7

19. Malik NM, Moore GBT, Smith G, Liu YL, Sanger GJ, Andrews PLR. Behavioural and hypothalamic molecular effects of the anti-cancer agent cisplatin in the rat: a model of chemotherapy-related malaise? *Pharmacol Biochem Behav.* 2006;83(1):9-20. doi:10.1016/j.pbb.2005.11.017

20. Álvarez Y, Pérez-Girón JV, Hernanz R, et al. Losartan reduces the increased participation of cyclooxygenase-2-derived products in vascular responses of hypertensive rats. *J Pharmacol Exp Ther.* 2007;321(1):381-388. doi:10.1124/jpet.106.115287

21. Huo X, Sun X, Cao Z, et al. Optimal ratio of 18α- and 18β-glycyrrhizic acid for preventing alcoholic hepatitis in rats. *Exp Ther Med.* 2019;18(1):172-178. doi:10.3892/etm.2019.7572

22. Khan IH, Krishnan VV, Ziman M, et al. Comparison of multiplex suspension array large-panel kits for profiling cytokines and chemokines in rheumatoid arthritis patients. *Cytometry B Clin Cytom.* 2009;76(3):159-168. doi:10.1002/cyto.b.20452

23. Harding SD, Sharman JL, Faccenda E, et al. The IUPHAR/BPS guide to PHARMACOLOGY in 2018: updates and expansion to encompass the new guide to IMMUNOPHARMACOLOGY. *Nucleic Acids Res.* 2018;46(D1):D1091-D1106. doi:10.1093/nar/gkx1121

24. Alexander SP, Fabbro D, Kelly E, et al. THE CONCISE GUIDE TO PHARMACOLOGY 2021/22: catalytic receptors. *Br J Pharmacol.* 2021;178(Suppl 1):S264-S312. doi:10.1111/bph.15541

25. Cameron AC, Touyz RM, Lang NN. Vascular complications of cancer chemotherapy. *Can J Cardiol.* 2016;32(7):852-862. doi:10.1016/j.cjca.2015.12.023

26. Ozkok A, Edelstein CL. Pathophysiology of cisplatin-induced acute kidney injury. *Biomed Res Int.* 2014;2014:1-17. doi:10.1155/2014/967826

27. Guglin M, Aljayeh M, Saiyad S, Ali R, Curtis AB. Introducing a new entity: chemotherapy-induced arrhythmia. *Europace.* 2009;11(12):1579-1586. doi:10.1093/EUROPACE/EUP300

28. Khan S, Chen CL, Brady MS, et al. Unstable angina associated with cisplatin and carboplatin in a patient with advanced melanoma. *J Clin Oncol.* 2012;30(18):e163-e164. doi:10.1200/JCO.2011.38.7852

29. Moore RA, Adel N, Riedel E, et al. High incidence of thromboembolic events in patients treated with cisplatin-based chemotherapy: a large retrospective analysis. *J Clin Oncol.* 2011;29(25):3466-3473. doi:10.1200/JCO.2011.35.5669

30. Ryberg M. Recent advances in cardiotoxicity of anticancer therapies. *Am Soc Clin Oncol Educ Book.* 2012;32:555-559. doi:10.14694/EDBOOK_AM.2012.32.40

31. Madeddu C, Deidda M, Piras A, et al. Pathophysiology of cardiotoxicity induced by nonanthracycline chemotherapy. *J Cardiovasc Med.* 2016;17:e12-e18. doi:10.2459/JCM.0000000000000376

32. Holditch SJ, Brown CN, Lombardi AM, Nguyen KN, Edelstein CL. Recent advances in models, mechanisms, biomarkers, and interventions in cisplatin-induced acute kidney injury. *Int J Mol Sci.* 2019;20(12):3011. doi:10.3390/ijms20123011

33. Chowdhury S, Sinha K, Banerjee S, Sil PC. Taurine protects cisplatin induced cardiotoxicity by modulating inflammatory and endoplasmic reticulum stress responses. *Biofactors.* 2016;42(6):647-664. doi:10.1002/biof.1301

34. Stojic IM, Zivkovic VI, Srejovic IM, et al. Cisplatin and cisplatin analogues perfusion through isolated rat heart: the effects of acute application on oxidative stress biomarkers. *Mol Cell Biochem.* 2018;439(1–2):19-33. doi:10.1007/s11010-017-3132-8

35. Aljuhani N, Ismail RS, El-Awady MS, Hassan MH. Modulatory effects of perindopril on cisplatin-induced nephrotoxicity in mice: implication

36. Deng JS, Jiang WP, Chen CC, et al. Cordyceps cicadae mycelia ameliorate cisplatin-induced acute kidney injury by suppressing the TLR4/NF-κB/MAPK and activating the HO-1/Nrf2 and Sirt-1/AMPK pathways in mice. *Oxid Med Cell Longev.* 2020;2020:1-17. doi:10.1155/2020/7912763

of inflammatory cytokines and caspase-3 mediated apoptosis. *Acta Pharm.* 2020;70(4):515-525. doi:10.2478/acph-2020-0033

37. Liang H, Liu HZ, Wang HB, Zhong JY, Yang CX, Zhang B. Dexmedetomidine protects against cisplatin-induced acute kidney injury in mice through regulating apoptosis and inflammation. *Inflamm Res.* 2017;66(5):399-411. doi:10.1007/s00011-017-1023-9

38. Guo Y, Wang M, Mou J, et al. Pretreatment of Huaiqihuang extractum protects against cisplatin-induced nephrotoxicity. *Sci Rep.* 2018;8(1):7333. doi:10.1038/s41598-018-25610-6

39. Barakat LAA, Barakat N, Zakaria MM, Khirallah SM. Protective role of zinc oxide nanoparticles in kidney injury induced by cisplatin in rats. *Life Sci.* 2020;262:118503. doi:10.1016/J.LFS.2020.118503

40. Khedr M, Barakat N, Mohey El-Deen I, Zahran F. Impact of preconditioning stem cells with all-trans retinoic acid signaling pathway on cisplatin-induced nephrotoxicity by down-regulation of TGFβ1, IL-6, and caspase-3 and up-regulation of HIF1α and VEGF. *Saudi J Biol Sci.* 2022;29(2):831-839. doi:10.1016/J.SJBS.2021.10.024

41. Wei C, Zhang Y, Zhong X, et al. Ginkgo biloba leaf extract mitigates cisplatin-induced chronic renal interstitial fibrosis by inhibiting the epithelial-mesenchymal transition of renal tubular epithelial cells mediated by the Smad3/TGF-β1 and Smad3/p38 MAPK pathways. *Chin Med.* 2022;17(1):25. doi:10.1186/S13020-022-00574-Y

42. Al Za'abi M, Al Salam S, Al Suleimani Y, et al. Effects of repeated increasing doses of cisplatin as models of acute kidney injury and chronic kidney disease in rats. *Naunyn Schmiedebergs Arch Pharmacol.* 2021;394(2):249-259. doi:10.1007/S00210-020-01976-1

43. Kursunluoglu G, Taskiran D, Kayali HA. The investigation of the antitumor agent toxicity and capsaicin effect on the electron transport chain enzymes, catalase activities and lipid peroxidation levels in lung, heart and brain tissues of rats. *Molecules.* 2018;23(12):3267. doi:10.3390/molecules23123267

44. Rosic G, Joksimovic J, Selakovic D, et al. The beneficial effects of sulfur-containing amino acids on Cisplatininduced cardiotoxicity and neurotoxicity in rodents. *Curr Med Chem.* 2018;25(3):391-403. doi:10.2174/0929867324666170705114456

45. Hsing CH, Tsai CC, Chen CL, et al. Pharmacologically inhibiting glycogen synthase kinase-3β ameliorates renal inflammation and nephrotoxicity in an animal model of cisplatin-induced acute kidney injury. *Biomedicine.* 2021;9(8):887. doi:10.3390/BIOMEDICINES9080887

46. Chen C, Ai Q, Wei Y. Hydroxytyrosol protects against cisplatin-induced nephrotoxicity via attenuating CKLF1 mediated inflammation, and inhibiting oxidative stress and apoptosis. *Int Immunopharmacol.* 2021;96:107805. doi:10.1016/J.INTIMP.2021.107805

47. Jing T, Liao J, Shen K, et al. Protective effect of urolithin a on cisplatin-induced nephrotoxicity in mice via modulation of inflammation and oxidative stress. *Food Chem Toxicol.* 2019;129:108-114. doi:10.1016/J.FCT.2019.04.031

48. El-Sheikh AAK, Khired Z. Morphine deteriorates cisplatin-induced cardiotoxicity in rats and induces dose-dependent cisplatin chemoresistance in MCF-7 human breast cancer cells. *Cardiovasc Toxicol.* 2021;21(7):553-562. doi:10.1007/S12012-021-09646-1

49. Nozaki Y, Kinoshita K, Yano T, et al. Signaling through the interleukin-18 receptor α attenuates inflammation in cisplatin-induced acute kidney injury. *Kidney Int.* 2012;82(8):892-902. doi:10.1038/KI.2012.226

50. Meng H, Fu G, Shen J, et al. Ameliorative effect of daidzein on cisplatin-induced nephrotoxicity in mice via modulation of inflammation, oxidative stress, and cell death. *Oxid Med Cell Longev.* 2017;2017:1-10. doi:10.1155/2017/3140680

51. Shen J, Wu JM, Hu GM, et al. Membrane nanotubes facilitate the propagation of inflammatory injury in the heart upon overactivation

of the β-adrenergic receptor. *Cell Death Dis*. 2020;11(11):1-11. doi:10.1038/s41419-020-03157-7

52. Xu J, Zhang B, Chu Z, Jiang F, Han J. Wogonin alleviates cisplatin-induced cardiotoxicity in mice via inhibiting gasdermin D-mediated pyroptosis. *J Cardiovasc Pharmacol*. 2021;78(4):597-603. doi:10.1097/FJC.0000000000001085

53. Zubowska M, Wyka K, Fendler W, Młynarski W, Zalewska-Szewczyk B. Interleukin 18 as a marker of chronic nephropathy in children after anticancer treatment. *Dis Markers*. 2013;35(6):811-818. doi:10.1155/2013/369784

54. Akhter J, Khan J, Baghel M, et al. NLRP3 inflammasome in rosma-rinic acid-afforded attenuation of acute kidney injury in mice. *Sci Rep*. 2022;12(1):1-15. doi:10.1038/s41598-022-04785-z

55. Aladaileh SH, Al-Swailmi FK, Abukhalil MH, Ahmeda AF, Mahmoud AM. Punicalagin prevents cisplatin-induced nephrotoxicity by attenuating oxidative stress, inflammatory response, and apoptosis in rats. *Life Sci*. 2021;286:120071. doi:10.1016/J.LFS.2021.120071

56. Thomas TP, Grisanti LA. The dynamic interplay between cardiac inflammation and fibrosis. *Front Physiol*. 2020;11:1133. doi:10.3389/fphys.2020.529075

57. Kong X, Wu S, Dai X, et al. A comprehensive profile of chemokines in the peripheral blood and vascular tissue of patients with Takayasu arteritis. *Arthritis Res Ther*. 2022;24(1):49. doi:10.1186/S13075-022-02740-X

58. Memi G, Yazgan B. Adropin and spexin hormones regulate the systemic inflammation in adenine-induced chronic kidney failure in rat. *Chin J Physiol*. 2021;64(4):194-201. doi:10.4103/CJP.CJP_13_21

59. Tang T, Gong T, Jiang W, Zhou R. GPCRs in NLRP3 inflammasome activation, regulation, and therapeutics. *Trends Pharmacol Sci*. 2018;39(9):798-811. doi:10.1016/j.tips.2018.07.002

60. Engin A. Endothelial dysfunction in obesity. *Adv Exp Med Biol*. 2017;960:345-379. doi:10.1007/978-3-319-48382-5_15

61. Michel HE, Menze ET. Tetramethylpyrazine guards against cisplatin-induced nephrotoxicity in rats through inhibiting HMGB1/TLR4/NF-κB and activating Nrf2 and PPAR-γ signaling pathways. *Eur J Pharmacol*. 2019;857:172422. doi:10.1016/j.ejphar.2019.172422

62. Li L, Tang W, Yi F. Role of inflammasome in chronic kidney disease. *Adv Exp Med Biol*. 2019;1165:407-421. doi:10.1007/978-981-13-8871-2_19

63. Gao R, Shi H, Chang S, et al. The selective NLRP3-inflammasome inhibitor MCC950 reduces myocardial fibrosis and improves cardiac remodeling in a mouse model of myocardial infarction. *Int Immunopharmacol*. 2019;74:105575. doi:10.1016/j.intimp.2019.04.022

64. Zhang Q, Sun Q, Tong Y, et al. Leonurine attenuates cisplatin nephrotoxicity by suppressing the NLRP3 inflammasome, mitochondrial dysfunction, and endoplasmic reticulum stress. *Int Urol Nephrol*. 2022;54:2275-2284. doi:10.1007/S11255-021-03093-1

65. Jiang S, Zhang H, Li X, et al. Vitamin D/VDR attenuate cisplatin-induced AKI by down-regulating NLRP3/Caspase-1/GSDMD pyroptosis pathway. *J Steroid Biochem Mol Biol*. 2021;206:105789. doi:10.1016/J.JSBMB.2020.105789

66. Juruj C, Lelogeais V, Pierini R, et al. Caspase-1 activity affects AIM2 speck formation/stability through a negative feedback loop. *Front Cell Infect Microbiol*. 2013;4:14. doi:10.3389/FCIMB.2013.00014/BIBTEX

67. Boza P, Ayala P, Vivar R, et al. Expression and function of toll-like receptor 4 and inflammasomes in cardiac fibroblasts and myofibro-blasts: IL-1β synthesis, secretion, and degradation. *Mol Immunol*. 2016;74:96-105. doi:10.1016/J.MOLIMM.2016.05.001

SUPPORTING INFORMATION

Additional supporting information can be found online in the Supporting Information section at the end of this article.